Desalination 502 (2021) 114928

Contents lists available at ScienceDirect

Desalination

journal homepage: www.elsevier.com/locate/desal

A zero liquid discharge system integrating multi-effect distillation and evaporative crystallization for desalination brine treatment

Qian Chen [a,*], Muhammad Burhan [a], Muhammad Wakil Shahzad [b], Doskhan Ybyraiymkul [a], Faheem Hassan Akhtar [a], Yong Li [c], Kim Choon Ng [a,*]

[a] Water Desalination and Reuse Center, King Abdullah University of Science and Technology, Thuwal 23955, Saudi Arabia
[b] Northumbria University, Newcastle upon Tyne, United Kingdom
[c] Institute of Refrigeration and Cryogenics, Shanghai Jiao Tong University, Shanghai 200240, China

HIGHLIGHTS

- A zero liquid discharged system is investigated for desalination brine treatment.
- Specific thermal energy consumption for per kg of brine is 600–1000 kJ.
- Overall Second-law efficiency spans 10–17%
- The cost of treating per m^3 of brine is $4.17 and is mainly contributed by thermal energy cost.

ARTICLE INFO

Keywords:
Zero liquid discharge
Multi-effect distillation
Evaporative crystallizer
Thermodynamic analysis
Techno-economic analysis

ABSTRACT

With growing global desalination capacity, brine from desalination plants has become an environmental threat to the ecosystems. One sustainable method for brine treatment is to develop zero liquid discharge systems that completely convert seawater into freshwater and salts. This paper presents a zero liquid discharge system, which consists of multi-effect distillation and evaporative crystallization, to treat desalination brine with a salinity of 70 g/kg. A thermodynamic analysis is firstly conducted for the proposed system. The specific heat consumption, specific heat transfer area, and Second-law efficiency are found to be 600–1100 kJ/kg, 110–340 m^2/(kg/s), and 10–17%, respectively. The heat consumption can be effectively reduced by increasing the number of MED stages, while the specific heat transfer area decreases significantly with higher heat source temperatures. Based on the thermodynamic performance, a techno-economic analysis is conducted for the proposed system, and the specific cost is calculated to be $4.17/$m^3$. Cost reduction can be achieved via employing cost-effective heat sources, reducing heat consumption, and scaling up the system. By selling the freshwater and salt crystals, the system will be more competitive than other existing brine treatment methods.

1. Introduction

Water scarcity has become one critical challenge due to the growth of world population and depletion of natural water sources. It is expected that global water scarcity will exceed 4000 billion m^3/year in 2030 [1], and more than 5 billion people will face water shortage [2]. To address the challenge of water crises, desalination has been extensively employed in areas with limited water supply. Desalination is the process of extracting freshwater from brackish water or seawater. Since 70% of the earth's surface is covered by the ocean, seawater desalination has the potential to provide an abundant freshwater supply. Over the past few decades, desalination has proved itself a promising and reliable solution to the global water deficit. More than 19,000 desalination plants have been installed worldwide, and global desalination capacity has reached 100 million m^3/day [3].

Most of the existing desalination processes, e.g., reverse osmosis (RO), multi-effect distillation (MED), and multi-stage flash desalination (MSF), can only separate a certain portion of freshwater (~50%) from seawater [4–6]. The remaining stream, which is named brine, has a higher salinity than regular seawater. Existing brine treatment methods usually discharge brine directly into the ocean or surface water [7,8]. They have many adverse effects on the environment. For example, direct brine discharge into the ocean will disturb the balance of the aquatic

* Corresponding authors.
E-mail addresses: chen_qian@u.nus.edu (Q. Chen), kimchoon.ng@kaust.edu.sa (K.C. Ng).

https://doi.org/10.1016/j.desal.2020.114928
Received 20 October 2020; Received in revised form 20 December 2020; Accepted 21 December 2020
Available online 11 January 2021

Nomenclature

A	area, m^2
BPE	boiling point elevation, °C
C	cost, $
$CAPEX$	capital expenditure, $/year
c_p	specific heat, J/kg
CRF	capital recovery factor
$\dot{D}$	distillate flowrate, kg/s
E	electricity, W
h	enthalpy, J/kg
h_{fg}	latent heat of vaporization, J/kg
i	interest rate, %
$\dot{m}$	mass flowrate, kg/s
MED	multi-effect distillation
N	number of MED stage
n	plant lifespan, year
$OPEX$	operational expenses, $/year
P	pressure, Pa
$pump$	pump
R	universal gas constant, J/mol-K
T	temperature, °C
t	time, year
U	overall heat transfer area, W/m^2-K
w	work, J
X	salinity, kg/kg
x	molar fraction, %

Greek letters

η	efficiency
Δ	difference
ρ	density, kg/m^3

Subscripts

a	species a
aeq	auxiliary equipment
b	brine; species b
bst	brine storage tank
C	crystallizer
cb	brine in crystallizer, before crystallization
$cb0$	brine in crystallizer, after crystallization
cc	capital cost
cf	circulating stream in crystallizer, after heating
$cf0$	circulating stream in crystallizer, before heating
ch	chemical
$cryst$	crystallizer
cw	cooling water
dcc	direct capital cost
eff	MED effect
el	electricity
f	feed
F	feed brine
fst	freshwater storage tank
h	heat source
H	heat source
i	ith stage
II	second-law
icc	indirect capital cost
la	labor
ls	land and site development
meq	main equipment
ot	other direct cost
re	plant replacement and maintenance
s	salt; saturation
$SEEC$	specific electricity consumption, J/kg
sep	separation
$STEC$	specific thermal energy consumption, J/kg
th	thermal energy
ut	utility cost
v	vapor
ZLD	zero liquid discharge

ecosystem and damage marine lives, while surface disposal may affect groundwater and soil quality [9,10].

One sustainable option for brine treatment is to develop zero liquid discharge (ZLD) systems that completely convert seawater into freshwater and salts. A ZLD system not only eliminates the need for brine disposal but also produces additional freshwater and valuable salts, thus increasing the value-add of the system. Several ZLD systems have been reported in the literature. Lu et al. [11] designed a ZLD system combining freeze desalination (FD), membrane distillation (MD), and freeze crystallization (FC). For a lab-scale system with a daily capacity of 72 kg, 50% of the heat can be supported by 50.5 m^2 of solar thermal collector, and 100% of the cooling power can be provided by regasification of 207 kg liquefied natural gas. Nakoa et al. [12] proposed a ZLD system consisting of direct contact membrane distillation (DCMD) and salinity gradient solar pond (SGSP). The system can deliver 52 L/day of freshwater per m^2 of membrane, and the energy consumption is 11 kW/m^2. Guo et al. [13] presented a flat-sheet air gap membrane distillation module (AGMD) coupled with an evaporative crystallizer for ZLD desalination. Energy consumption for treating per kg of brine was found to be 1651.5 kJ. Guan et al. [14] analyzed a membrane distillation crystallization system for brine treatment. 97.8% of energy was consumed in the MD heater, and heat recovery from the permeate stream could increase the thermal efficiency by 28%. Julian et al. [15] studied the effect of operation parameters on the performance of a submerged vacuum membrane distillation-crystallization system. Both transverse vibration and aeration were found to increase the flux at the beginning, but rapid flux reduction was observed for transverse vibration due to enhanced $CaCO_3$ precipitation.

Most of the above-mentioned ZLD systems employ MD for brine concentration, which is an extension of emerging research interests in MD desalination systems. However, MD systems will face serious membrane scaling and fouling when treating brine with high salinity, which will lead to serious performance degradation [16,17]. Comparing to MD, conventional MED has better stability when treating highly concentrated solutions, which reduces maintenance and operational requirements. MED also has better energy efficiency and larger treatment capability over MD. Therefore, the efficacy of conventional MED systems in brine treatment has also been the subject of great research interests. Zhao et al. [18] analyzed a MED system for high-salinity wastewater desalination. Results revealed that more numbers of MED stages promoted energy efficiency at the expense of higher initial costs, while higher steam temperatures reduced the required heat transfer area. Panagopoulos [19] conducted a techno-economic analysis on a multi-effect distillation/thermal vapor compression system (MED-TVC) for brine concentration. The freshwater cost was found to be $1.69/$m^3$ under the scenario of waste heat utilization. Shahzad et al. [4] proposed a hybrid multi-effect adsorption distillation (MEAD) system for treating RO brine. An overall recovery ratio of 80% was achieved with a specific electricity consumption of 1.76 kWh/m^3. Onishi et al. [20] integrated a MED system with mechanical vapor recompression (MVC) for brine concentration. The salinity of brine reached 300 g/kg under different design and operating conditions, thus allowing the achievement of ZLD

status.

From the above review, it can be noted that most of the existing studies on MED for brine concentration focused on concentrating the brine to near saturation. To achieve a real ZLD status, further processing of the concentrated brine, e.g. crystallization, is necessary to completely separate water and salts. However, little attention is paid to the crystallization process in the existing studies. Comparing with a stand-alone MED system, the hybrid MED-crystallization process requires special design and operation to achieve the ZLD status, but such information is not available in the literature. Also, crystallization consumes significant amounts of energy and induces additional initial and operational costs, while thermodynamic and techno-economic analyses on the hybrid MED-crystallization process have yet to be conducted.

To address existing knowledge gaps, this paper presents a systematic study on a hybrid MED-crystallization system for desalination brine treatment. A thermodynamic analysis will be conducted first to obtain the optimal feed brine flowrate to achieve ZLD status under different design and operating conditions. The corresponding energy (heat and electricity) consumption, specific heat transfer area, and Second-law efficiency will also be investigated. Afterward, an economic analysis will be performed to calculate the cost of the proposed process. The impacts of key parameters will also be analyzed to identify the major cost drivers and explore viable solutions for cost reduction. Finally, a comparison with other existing brine management methods will be presented to highlight the economic competitiveness of the proposed system. The novelty and originality of this study are summarized as follows: (1) a more advanced ZLD system with higher stability and reliability, better energy efficiency, and better capability of renewable energy utilization, is proposed and evaluated; (2) an in-depth thermodynamic analysis that covers energetic and Second-law efficiencies is conducted to for the hybrid ZLD system considering the interactions of different subsystems; and (3) an economic analysis is presented to evaluate the economic viability of ZLD. The results will provide useful insights into the design and operation of the ZLD system consisting of MED and evaporative crystallization.

2. Process description

The proposed ZLD system consists of a MED system and an evaporative crystallizer. The MED is arranged in a forward-feed manner so that maximum concentration occurs in the last effect that has the lowest temperature and the risks of scaling and fouling are minimized. The evaporative crystallizer consists of a heater, an evaporation/crystallization chamber, a salt/brine separation device, and a condenser. Brine from a regular desalination plant is firstly concentrated in the MED system, and then the concentrated brine is directed to the crystallizer for complete separation of salt and water.

Fig. 1 shows the schematic of the proposed ZLD system. Feed brine is sprayed into the cold side of the first MED stage, and an external heat source (e.g. steam or hot water) is supplied to the tube side of the first

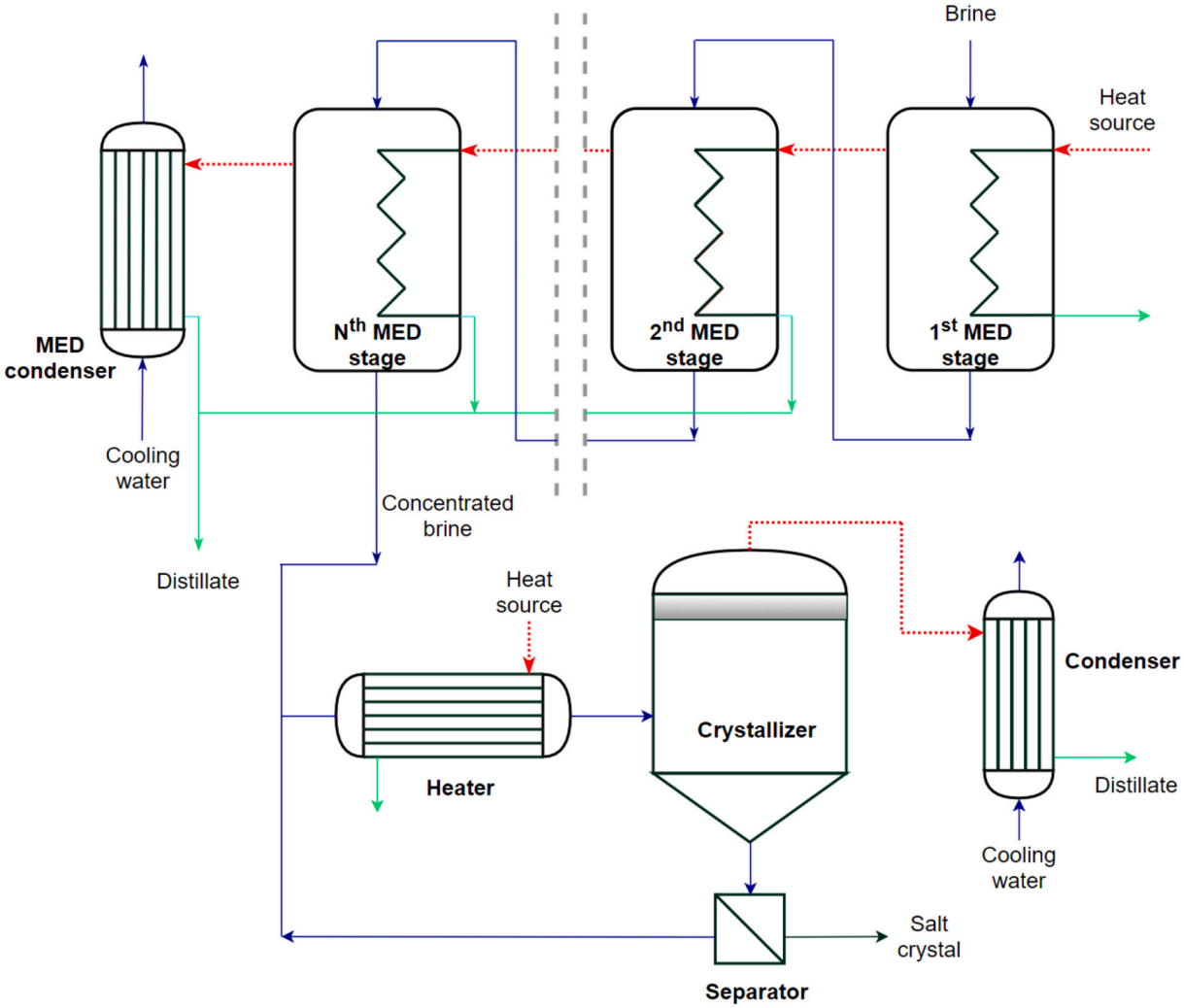

Fig. 1. Schematic diagram of the zero liquid discharge system integrating a MED and an evaporative crystallizer.

stage to heat up and partially evaporate the feed brine. The produced vapor is directed to the tube side of the second stage, while the unevaporated brine at the bottom of the first stage constitutes the feed stream of the second stage. The second MED stage has a lower pressure than the first one so that vapor from the first stage can be condensed, and the condensation heat is transferred to the feed brine to induce evaporation. The process is repeated in the following stages, and vapor produced in the last stage is condensed in an external condenser. The brine leaving the last MED stage is mixed with the recirculation stream of the crystallizer. After that, the mixed stream is heated and injected into the crystallization chamber that is under vacuum condition. In the chamber, a portion of the hot stream flashes off and the salt concentration exceeds the solubility limit. Thus salt precipitation takes place at the bottom of the chamber. Salt crystals are separated from the brine slurry using a separator (e.g. centrifuge), and the flashed vapor is condensed in an external condenser to sustain the vacuum level in the crystallization chamber.

Comparing with the ZLD systems reported in the literature, the proposed system possesses several advantages. Firstly, MED is used for brine concentration, which has better stability and higher energy efficiency than MD systems. Secondly, since the evaporative crystallizer can further concentrate the brine, the brine leaving the previous process doesn't have to be supersaturated, and the potential of scaling and fouling in the brine concentrator (i.e., MED) can be significantly reduced. Thirdly, both MED and evaporative crystallizer can handle large brine flowrates, making the system capacity larger than those based on MD and solar ponds. Finally, the system allows the implementation of various low-grade heat sources, e.g. solar thermal energy and industrial waste heat, thus making the process more sustainable and environmentally friendly.

3. Mathematical modelling

The thermodynamic and thermo-economic performances of the proposed ZLD system are evaluated via mathematical modelling. A process model is firstly developed to access its thermodynamic efficiency and specific heat transfer area under different design and operation conditions. Based on the results of the thermodynamic analysis, an economic model is derived to obtain the final cost of the ZLD system for treating unit mass of brine.

3.1. Process model

The mathematical model for MED is derived based on the schematic diagram shown in Fig. 2(a). The subscript "i" represents the ith MED stage (totally N stages). Subscripts f, h, and b are the feed, heating, and brine streams, respectively. $\dot{m}$ is the mass flowrate of water and heating steam, and $\dot{D}$ is the flowrate of the produced vapor. These symbols will be employed in the model equations. The following assumptions are made for the MED model:

(1) The system is under steady-state;
(2) Heat loss to the ambient is negligible;
(3) The distillate is salt-free;
(4) Vapor is completely condensed at the saturation temperature;
(5) Properties for seawater and vapor are constant in each stage, and they are derived based on temperature, pressure, and salinity in the corresponding stage.

Table 1 summarizes the equations for MED. Specifically, Eqs. (1)–(3) describe heat and mass balance in each stage, Eqs. (4) & (5) represent heat transfer, while Eqs. (6) & (7) are energy balance and heat transfer in the condenser. Eqs. (8)–(11) are the inlet conditions for feed flowrate, feed concentration, heat source temperature, and heat source flowrate, respectively. The pumping power is calculated in Eq. (12). The

Table 1
Process model for MED.

Equation	No.	Description
$\dot{m}_{f,i} = \dot{m}_{b,i} + \dot{D}_i$	(1)	MED effect mass balance;
$\dot{m}_{b,i}X_{b,i} = \dot{m}_{f,i}X_{f,i}$	(2)	MED effect salt balance;
$\dot{m}_{h,i}h_{fg} = \dot{D}_i h_{fg} + \dot{m}_{b,i}h_b - \dot{m}_{f,i}h_f$	(3)	MED effect energy balance;
$\dot{m}_{h,i}h_{fg} = UA(T_{h,i} - T_{b,i})$	(4)	MED effect heat transfer;
$T_{b,\,i} = T_{v,\,i} + BPE(X_{f,\,i})$	(5)	Boiling point elevation of seawater;
$\dot{m}_{cw}c_p(T_{cw,o} - T_{cw,i}) = \dot{D}_N h_{fg}$	(6)	MED condenser heat balance;
$T_{cw,o} = T_{v,N} - (T_{v,N} - T_{cw,i})exp\left(-\frac{UA}{\dot{m}_{cw}c_p}\right)$	(7)	MED condenser heat transfer;
$\dot{m}_{f,i} = \begin{cases} \dot{m}_{b,i-1}, i \neq 1 \\ \dot{m}_F, i = 1 \end{cases}$	(8)	Feed flowrate in each effect;
$\dot{m}_{h,i} = \begin{cases} \dot{D}_{i-1}, i \neq 1 \\ \dot{m}_{h,MED}, i = 1 \end{cases}$	(9)	Heating steam flowrate in each effect;
$T_{f,i} = \begin{cases} T_{b,i-1}, i \neq 1 \\ T_F, i = 1 \end{cases}$	(10)	Heating steam temperature in each effect;
$X_{f,i} = \begin{cases} X_{b,i-1}, i \neq 1 \\ X_F, i = 1 \end{cases}$	(11)	Feed salinity in each effect;
$\dot{E}_{MED} = \sum \frac{\dot{m}_i \Delta P_i}{\dot{\rho}_i \eta_{pump}}$	(12)	Overall electricity consumption in MED;

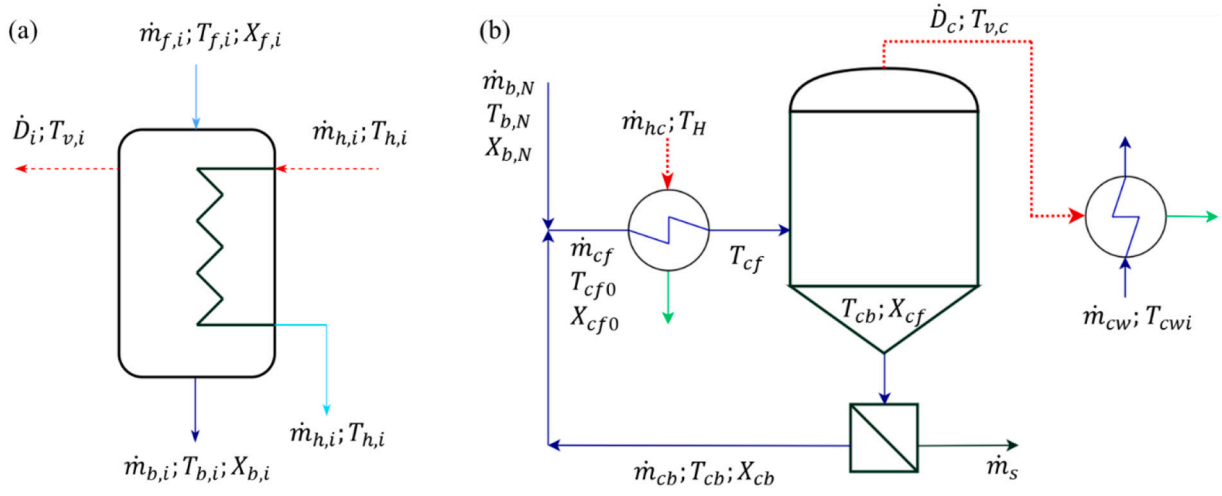

Fig. 2. Model schematic for (a) MED stages and (b) crystallizer with major symbols.

properties of seawater and vapor are derived using the equations presented in [21–23], while heat transfer coefficients are calculated using the correlations reported in [24].

The model schematic for the crystallizer is shown in Fig. 2(b). Similar to MED, the crystallizer is modelled based on steady-state analysis on heat and mass balances, and heat losses to the environment are neglected. Table 2 summarizes the model equations for the crystallizer. The global mass balances for water and salt are derived in Eqs. (13) & (14), mixing of the MED brine and the recirculation stream are modelled using Eqs. (15)–(17), and the heating process is depicted by Eqs. (18) & (19). Eqs. (20) & (21) describe the flash evaporation process. Eqs. (22)–(25) describe the crystallization process with a crystallization ratio of R_c [25]. For simplicity, only NaCl salt is considered during the crystallization process, as it represents the main salt content in seawater. Eqs. (26)–(28) are energy balances in the crystallizer condenser, and Eq. (29) calculates the pumping power consumption of the crystallizer.

To evaluate the thermodynamic performance of the ZLD system, several performance indicators are introduced, including: (1) specific thermal energy consumption (*STEC*), the heat consumption for treating unit mass of brine, (2) specific electricity consumption (*SEEC*), the electricity consumption for treating unit mass of brine, (3) specific heat transfer area (*sA*), the required heat transfer area for treating unit mass of brine, and (4) Second-law efficiency, the ratio of exergy output to exergy input. Expressions for these parameters are provided in Table 3. The minimum work of separation, which represents the minimum work for completely separating salt and water, is adopted from [26,27].

3.2. Economic model

Table 4 summarizes the euqations for economic evaluation. The total cost for brine treatment includes capital costs and annual operating costs. Capital costs, also called capital expenditure (*CAPEX*), consist of direct and indirect capital costs. Direct capital costs contain equipment (e.g. MED, crystallizer, feed tank, freshwater tank, etc.) procurement costs, land costs, site development costs, and installation costs, which are expressed in Eq. (35). Indirect capital costs include freight, insurance, and contingency costs. They are usually estimated as a percentage of the direct capital costs [28], as expressed in Eq. (36). Annual operating costs are also called operating expenses (OPEX), and they include the energy (thermal and electricity) costs, labor costs, chemical costs, maintenance costs, and equipment replacement costs. Detailed expression of the OPEX is given in Eq. (40).

Table 2
Process model for crystallizer.

Equation	No.	Description
$\dot{D}_C = \dot{m}_{b,N}(1 - X_{b,N})$	(13)	Distillate flowrate in crystallizer;
$\dot{m}_s = \dot{m}_{b,N} X_{b,N}$	(14)	Salt crystal mass flowrate in crystallizer;
$\dot{m}_{cf} = \dot{m}_{b,N} + \dot{m}_{cb}$	(15)	Mixing of feed and recirculation steams;
$\dot{m}_{cf} X_{cf} = \dot{m}_{b,N} X_b + \dot{m}_{cb} X_{cb}$	(16)	Salt balance of mixing;
$\dot{m}_{cf} h_{cf} = \dot{m}_{b,N} h_b + \dot{m}_{cb} h_{cb}$	(17)	Energy balance of mixing;
$T_{cf} = T_H - (T_H - T_{cf0}) exp\left(-\frac{UA}{\dot{m}_{cf} c_p}\right)$	(18)	Heat transfer in crystallizer heater;
$\dot{m}_{hc} h_{fg} = \dot{m}_{cf} c_p (T_{cf} - T_{cf0})$	(19)	Energy balance in crystallizer heater;
$\dot{D}_c h_{fg} = \dot{m}_{cf} c_p (T_{cf} - T_{cb0})$	(20)	Flash evaporation in crystallizer;
$\left(\dot{m}_{cf} - \dot{D}_C\right) X_{cf} = \dot{m}_{cf} X_{cf0}$	(21)	Salt balance after flash evaporation;
$\dot{m}_s = \left(\dot{m}_{cf} - \dot{D}_C\right) R_c (X_{cf} - X_s)$	(22)	Salt crystallization, with a crystallization ratio of R_c;
$X_s = 0.2628 + 62.75 \times 10^{-6} T_{cb} + 1.08 \times 10^{-6} T_{cb}^2$	(23)	Saturation salt concentration;
$\dot{m}_{cb} X_{cb} = \dot{m}_{cf} X_{cf0} - \dot{m}_s$	(24)	Salt balance during crystallization;
$\left(\dot{m}_{cf} - \dot{D}_C\right) c_p (T_{cb} - T_{cb0}) = \dot{m}_s \Delta h_{cryst}$	(25)	Energy balance during crystallization;
$T_{cb} = T_{v,\,cryst} + BPE(X_{cf})$	(26)	Boiling point elevation in crystallizer;
$\dot{m}_{cw} c_p (T_{cw.o} - T_{cw.i}) = \dot{D}_C h_{fg}$	(27)	Energy balance in crystallizer condenser;
$T_{cw,o} = T_{v,cryst} - (T_{v,cryst} - T_{cw,i}) exp\left(-\frac{UA_{cryst}}{\dot{m}_{cw} c_p}\right)$	(28)	Heat transfer in crystallizer condenser;
$\dot{E}_{cryst} = \frac{\dot{m}_{cf} \Delta P_{cf}}{\dot{\rho}_{cf} \eta_{pump}} + \frac{\dot{m}_{cw} \Delta P_{cw}}{\dot{\rho}_{cw} \eta_{pump}}$	(29)	Overall electricity consumption in crystallizer;

Table 3
Performance indicators for the ZLD system.

Equation	No.	Description
$STEC = \frac{\left(\dot{m}_{h,MED} + \dot{m}_{h,C}\right) h_{fg}}{\dot{m}_F}$	(30)	Specific thermal energy consumption;
$SEEC = \frac{\dot{E}_{cryst} + \dot{E}_{MED}}{\dot{m}_F}$	(31)	Specific electricity consumption;
$sA = \frac{NA_{eff} + A_{c,MED} + A_{h,cryst} + A_{c,cryst}}{\dot{m}_F}$	(32)	Specific heat transfer are;
$\eta_{II} = \frac{\dot{m}_F w_{sep}}{\left(\dot{m}_{hm} + \dot{m}_{hc}\right) h_{fg}(1 - T_0/T_H) + \dot{E}_{cryst} + \dot{E}_{MED}}$	(33)	Second-law efficiency;
$w_{sep} = \frac{-nRT[x_a ln(x_a) + x_b ln(x_b)]}{m_F}$	(34)	Least work of separation;

Table 4
Economic model of the system.

Component	Equation	No.
Direct capital cost	$C_{dcc} = C_{meq} + C_{aeq} + C_{ls} + C_{bst} + C_{fst} + C_{ut} + C_{ot}$	(35)
Indirect capital cost	$C_{icc} = 10\,\% \times C_{dcc}$	(36)
Total capital cost	$C_{cc} = C_{icc} + C_{dcc}$	(37)
Capital recovery factor	$CRF = \frac{i(1+i)^n}{(1+i)^n - 1}$	(38)
Annual capital cost	$CAPEX = C_{cc} \times CRF$	(39)
Operating costs	$OPEX = C_{th} + C_{el} + C_{la} + C_{ch} + C_{re}$	(40)
Specific cost	$C_{ZLD} = \frac{CAPEX + OPEX}{\dot{m}_F \times t}$	(41)

3.3. Solution algorithm

The model equations are formulated and solved using MATLAB. Based on the design and operating data, the MED model is solved first to get the flowrate, concentration, and temperature of the brine as the input of the crystallizer. Afterward, the crystallization process is simulated to get the energy (heat and electricity) consumption and required heat transfer area for the crystallizer as well as the whole system. Finally, the results of the thermodynamic analysis are employed in the economic model to obtain the cost for the whole ZLD system. The solution algorithm is illustrated in Fig. 3.

4. Results and discussion

In this section, the thermodynamic performance of the hybrid ZLD system will be evaluated first using the developed model. Particularly, the impacts of several design and operating parameters, including the feed brine flowrate, the number of MED stages, and the heat source temperature, will be investigated. Then the results of the thermodynamic analysis will be used in the economic analysis to calculate the plant cost. Finally, possible solutions to optimize the ZLD system will be proposed and discussed.

4.1. Thermodynamic analysis

The mathematical model is firstly validated using operation data of

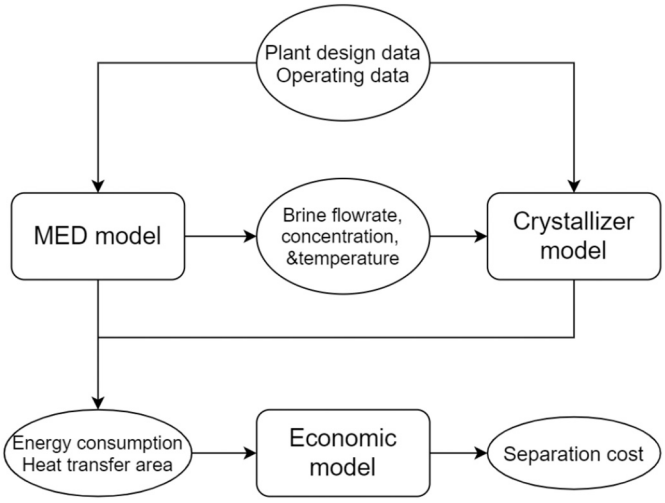

Fig. 3. Solution algorithm for the thermodynamic and thermo-economic model.

the pilot MED plant at Plataforma Solar de Almería (PSA) [29]. The comparison reveals that the model is capable of predicting the production rate, energy efficiency, and the required heat transfer area with high accuracy. Detailed information for validation is provided in the Supplementary Material.

After validation, the process model is employed to evaluate the performance of the proposed ZLD system. Specifically, the impacts of feed flowrate, the number of MED stages, and the heat source temperature will be investigated. Although the effects of these parameters on MED performance have been extensively studied in the literature, very few works discuss their effects on a hybrid system that aims at achieving ZLD status. For illustration purposes, the feed brine salinity and temperature are assumed to be 70 g/kg and 30 °C, respectively. Other thermodynamic data used in the simulations are provided in Table 5.

4.1.1. Energetic analysis

An energetic analysis is firstly presented by evaluating the consumption of heat and electricity under different conditions. Without loss of generality, the reference condition is considered to have 5 MED stages, a feed flowrate of 0.75 kg/s, and a heat source temperature of 75 °C.

Fig. 4 shows the impact of the feed brine flowrate on the energy consumption of the proposed ZLD system. As can be seen from Fig. 4(a), heat consumption in the crystallizer becomes higher when increasing the feed flowrate, leading to a higher specific heat consumption for the ZLD system. The reason is that when the feed flowrate is higher, more brine has to be treated in the crystallizer to achieve ZLD status. Since the crystallizer has no internal heat recovery, it takes more heat to evaporate the same amount of water than in MED. Consequently, overall heat consumption at the system level is higher when the feed flowrate is increased.

Fig. 4(b) shows electricity consumption under different feed flowrates. The value firstly decreases when increasing the feed flowrate, and the trend is reversed when the feed flowrate is higher than 0.74 kg/s. The reason can be explained as follows. On the one hand, the cooling water flowrate is fixed in the condensers. When the feed flowrate is higher, specific electricity consumption for cooling water pumping becomes less significant, as demonstrated by a decreasing electricity consumption in MED. On the other hand, more amount of water needs to be evaporated in the crystallizer, and recirculation flowrate in the crystallizer (shown in Fig. 4(c)) increases exponentially with feed flowrate, leading to more pumping power consumption. The final trend is the result of the trade-off between these two competing effects.

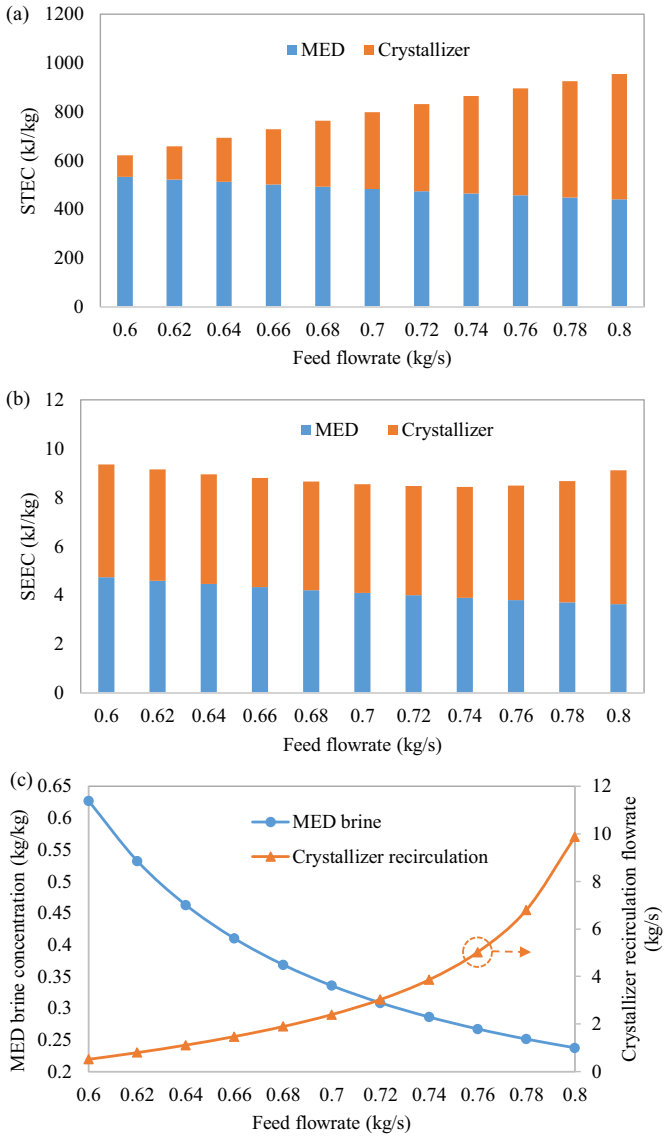

Fig. 4. (a) Specific heat consumption, (b) specific electricity consumption, and (c) MED brine concentration and crystallizer recirculation flowrate under different feed flowrates with 5 MED stages and heat source temperature of 75 °C.

Table 5
Thermodynamic assumptions for the simulations.

Parameter	Unit	Value
Feed brine salinity, X_F	g/kg	70
Feed brine temperature, T_F	°C	30
Feed brine flowrate, $\dot{m}_F$	kg/s	0.6–0.8
Number of MED stages, N	–	3–10
Heat source temperature, T_H	°C	55–80
Feed pressure drop in MED effects, ΔP_f	bar	0.5
Cooling water pressure drop in MED condenser, $\Delta P_{c,MED}$	bar	2
MED distillate extraction pressure drop, $\Delta P_{d,MED}$	bar	0.5
Crystallizer circulation pressure drop, ΔP_{cf}	bar	1.5
Cooling water pressure drop in crystallizer condenser, ΔP_{cw}	bar	2
Crystallizer distillate extraction, $\Delta P_{d,C}$	bar	0.5
Pumping efficiency, η	%	75
Crystallization ratio, R	%	90
UA in MED effects	W/K	50,000
UA in MED condenser	W/K	50,000
UA in crystallizer heater	W/K	25,000
UA in crystallizer condenser	W/K	25,000

From the thermodynamic point of view, a lower feed flowrate is preferable to achieve higher energy efficiency. However, during practical operations, the minimum feed flowrate is limited by the brine concentration. As shown in Fig. 4(c), when the feed flowrate is lower, the brine leaving the last MED stage has higher salinity, and the risks for scaling and fouling become higher. To avoid such risks, it is recommended that the feed flowrate is >0.76 kg/s so that the brine concentration does not exceed 0.26 kg/kg (the saturation concentration corresponding to the temperature in the last stage). The corresponding specific thermal energy consumption is 895–955 kJ/kg under such flowrate range. The value is lower than that of MD-based ZLD systems reported in the literature (e.g. >2000 kWh/m^3 in [11], 1651 kJ/kg in [13]), which is attributed to more effective heat recovery in the MED system.

Fig. 5(a) and (b) show the energy consumption under different numbers of MED stages. The brine concentration leaving MED is controlled to be 0.26 kg/kg, and the corresponding feed flowrates are provided in Fig. 5(c). As can be expected, heat consumption in MED drops remarkably with more MED stages, since the recovery of condensation heat is more effective. When the number of stages increases from 3 to 10, specific heat consumption in MED is reduced by ~60% (from 680 to 288 kJ/kg), and thermal energy saving at the system level is ~34%. On the other hand, the change of pumping power is relatively small (±5%) for different MED designs, and its value is inversely proportional to the feed flowrate. Although more power is required for feed injection when MED has more stages, feed flowrate is much smaller than cooling water flowrate (0.6–0.8 kg/s vs 20 kg/s), and pressure drops for feed streams (0.5 bar) are also lower than that of cooling water (2 bar). Therefore, specific electricity consumption benefits from less pumping power for cooling water when the feed flowrate is higher.

Fig. 6 (a) and (b) show the impact of heat source temperature on energy efficiency. The corresponding feed flowrate that gives a MED brine concentration of 0.26 kg/kg is provided in Fig. 6(c). As shown in Fig. 6(a), the thermal energy consumption increases slightly when the heat source temperature is higher, which can be attributed to a higher latent heat of vaporization under higher temperatures. In contrast, the pumping power consumption is reduced markedly under a higher heat source temperature. For fixed cooling water temperature, a higher heat

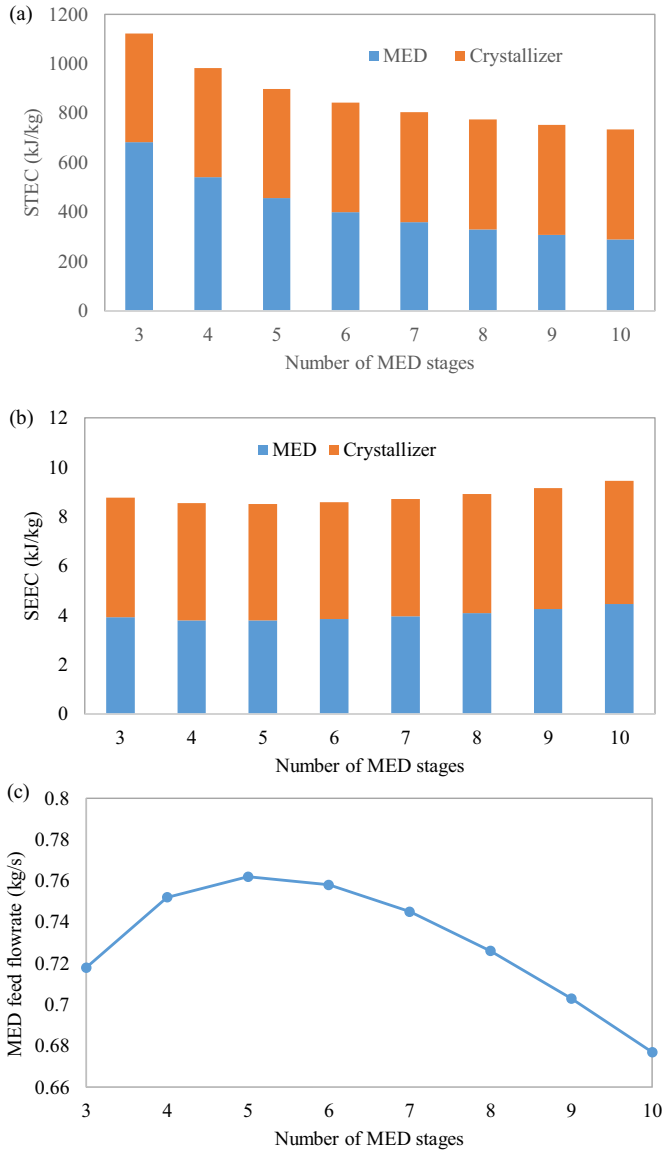

Fig. 5. (a) Specific heat consumption, (b) specific electricity consumption, and (c) MED feed flowrate under different numbers of MED stages with a heat source temperature of 75 °C.

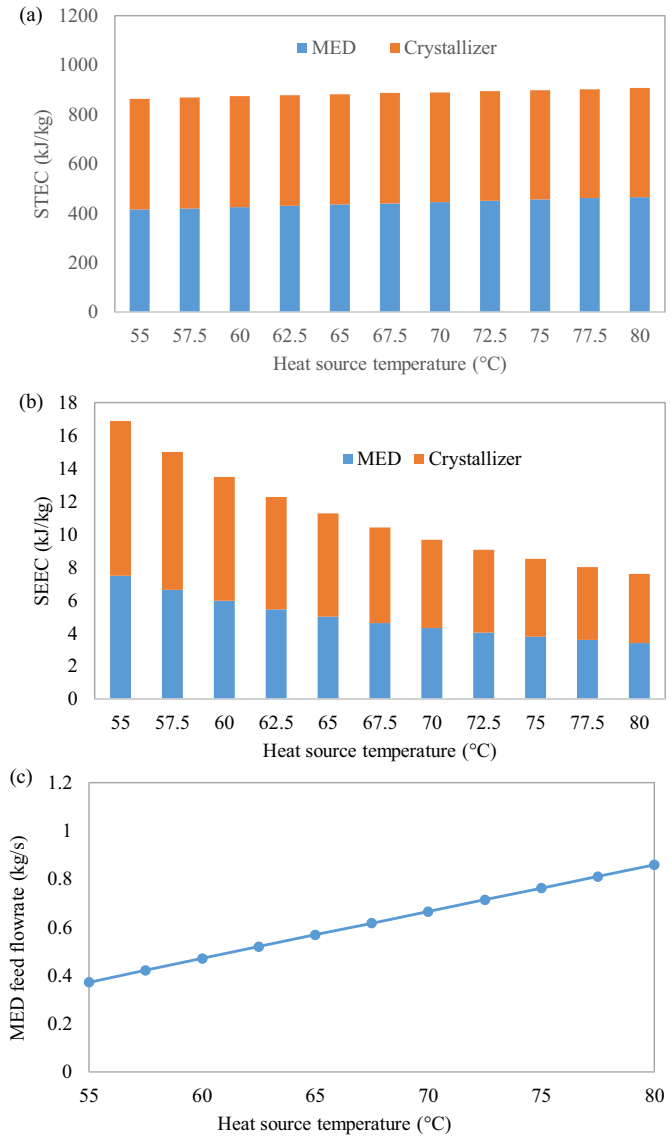

Fig. 6. (a) Specific heat consumption, (b) specific electricity consumption, and (c) MED feed flowrate under different heat source temperatures with 5 MED stages.

source temperature provides a larger driving force for evaporation, thus allowing more brine to be treated, as can be seen from Fig. 6(c). Consequently, specific pumping power of cooling water gets smaller, as addressed previously, leading to less electricity consumption for treating unit mass of brine.

4.1.2. Specific heat transfer area

Specific heat transfer area is another key parameter for thermal desalination systems, as it is directly correlated with the initial plant costs. Fig. 7 depicts the specific heat transfer area under different design and operating conditions. For a given system, the specific heat transfer area for unit mass of feed brine decreases when more feed is supplied to the system, as shown in Fig. 7(a). On the other hand, when the feed flowrate is constant, the specific area becomes higher when more heat transfer area is provided, i.e. MED has more stages, as depicted in Fig. 7 (b). Specific heat transfer area also decreases under higher heat source temperatures, as can be seen in Fig. 7(c), because the driving force for heat transfer is larger.

It is also interesting to note that the specific heat transfer area is smaller than that of the stand-alone MED system reported in [24]. This is because all evaporation occurs on the heat exchanger surface for the stand-alone MED system, while in the proposed ZLD system a large portion of vapor is produced by flash evaporation in the crystallization chamber without any metallic surface for heat transfer.

4.1.3. Second-law efficiency

The specific energy consumption provides the quantity of energy input during actual operations, while the quality of energy sources is not revealed. On the other hand, the Second-law efficiency provides deeper thermodynamic insights and demonstrates how far a thermal system deviates from its thermodynamic limit [30–32]. Fig. 8 shows the Second-law efficiency of the proposed ZLD system under different design and operating conditions. Obviously, the Second-law efficiency is higher under a lower feed flowrate and more numbers of MED stages. The same conditions also lead to lower specific heat consumption, indicating less exergy input. The Second-law efficiency also increases with a lower heat source temperature, although the specific heat consumption is marginally affected by the heat source temperature. This is because the quality of thermal energy is lower when it is at a lower temperature, which

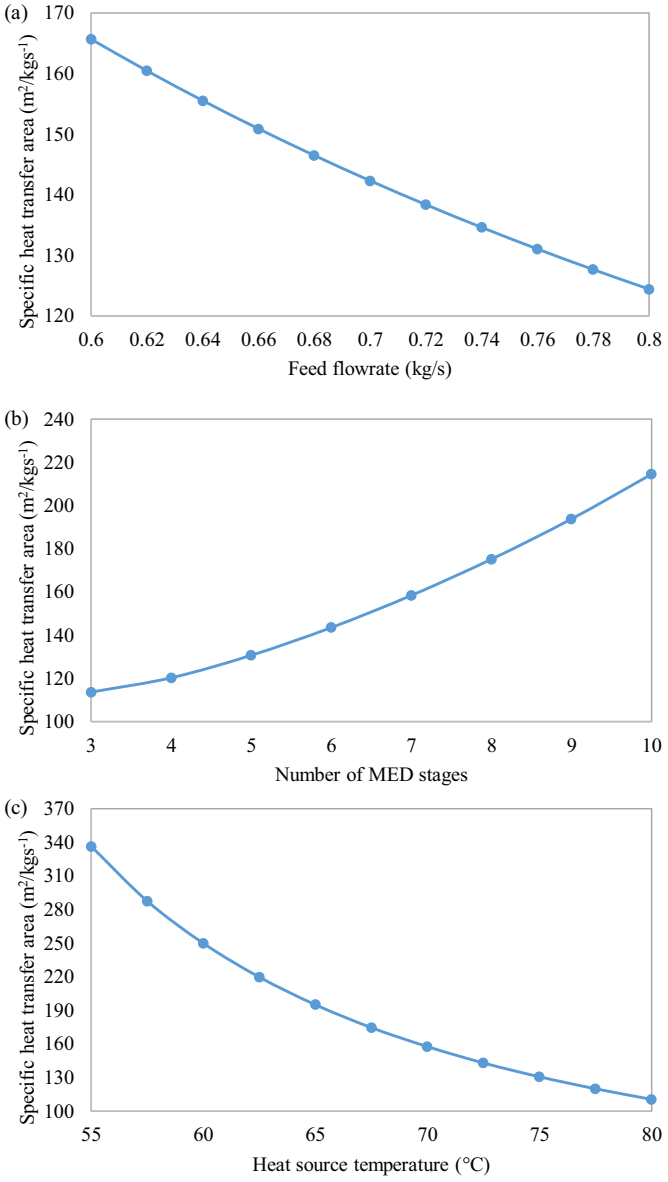

Fig. 7. Effects of different parameters on specific heat transfer: (a) feed flowrates, (b) total number of MED stages, and (c) heat source temperatures.

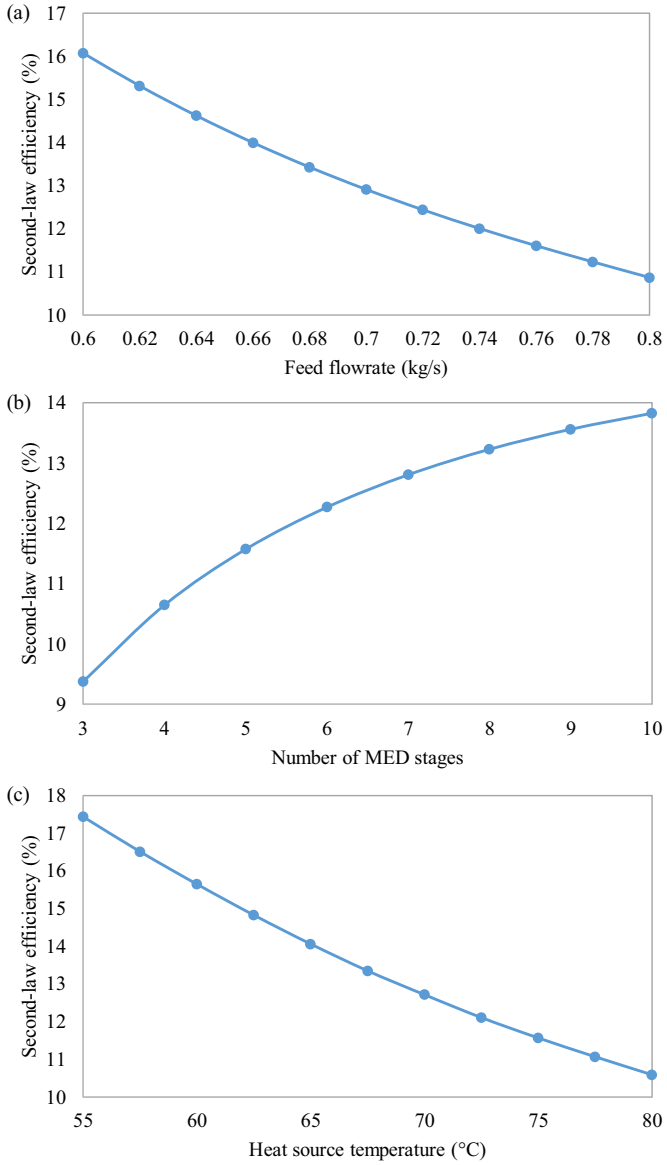

Fig. 8. Second-law efficiency under (a) different feed flowrates, (b) total number of MED stages, and (c) heat source temperatures.

translates into less exergy consumption.

It is also worth mentioning that the Second-law efficiency of the proposed ZLD system is higher than regular thermal desalination systems [31–33], although more energy is consumed. This can be explained by a higher work of separation for ZLD. As depicted in Fig. 9, the minimum work of separation gets higher when the recovery ratio increases. To achieve ZLD status, the recovery ratio approaches 100%, and the corresponding separation work is four times higher than that under a vanishing recovery ratio. A higher separation work translates into more exergy output and higher Second-law efficiency for the ZLD system.

4.2. Economic analysis

From the above analysis, it can be found that the energy efficiency is improved at the expense of increasing the heat transfer area, which leads to higher plant initial costs. Therefore, the economic viability of increasing the heat transfer area is subjected to the relative costs of equipment and energy. In this section, a detailed economic performance is performed for the proposed system. The economic data is provided in Table 6. These data are acquired from the open literature [34–37] as well as quotations from the manufacturer.

Fig. 10 illustrates the contribution of different cost components to *CAPEX* and *OPEX* for a ZLD system with 5 MED stages, a heat source temperature of 75 °C and a feed brine flowrate of 0.75 kg/s. It is revealed that the MED plant, the crystallizer, and the storage tanks (feed tank and distillate tank) are the main cost drivers for *CAPEX*, whereas thermal energy cost contributes >90% of the *OPEX*. Moreover, the *OPEX* is several times higher than the *CAPEX*, making the thermal energy cost the main contributor to the final cost ($4.17/m^3).

The final cost is expected to decrease when thermal energy with low cost is available. As revealed in Fig. 11(a), the final cost decreases almost linearly with the drop in thermal energy price. Under the ideal situation, thermal energy cost can be completely eliminated by employing waste heat, and the final cost can be markedly reduced to $1.16/m^3. The final cost can also be lowered by scaling up the plant since the fixed costs can be spread to more units of products, as can be seen from Fig. 11(b). Two scenarios are considered here, namely, (1) the regular scenario with a steam price of $8/ton, and (2) the waste heat recovery scenario with negligible thermal costs. Under both scenarios, the specific cost can be reduced by $0.3/m^3 via expanding the plant capacity from 20 to 400 m^3/day, after which the economic benefit of scaling up diminishes.

Under the regular scenario, the cost of thermal energy can be reduced by improving the system's energy efficiency, i.e. reducing feed flowrates and increasing heat source temperatures, as shown in Fig. 12 (a)&(b). Increasing the number of MED stages also reduces heat consumption, but it is achieved at the expense of higher plant costs. Consequently, the final cost starts to increase when there are more than eight stages, as plotted in Fig. 12(c). On the other hand, when waste heat with negligible costs is available, thermal energy cost is no longer a concern, and the final cost will be lower when productivity is higher or initial plant cost is lower, i.e., higher feed flowrate, higher heat source temperature, and fewer MED stages, as given by orange lines in Fig. 12.

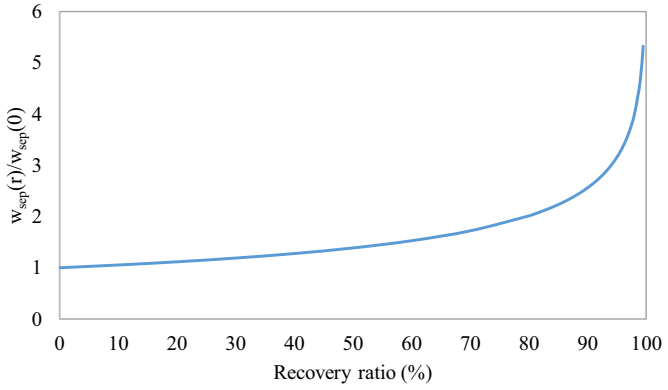

Fig. 9. Minimum work of separation under different recovery ratio.

Table 6
Economic data for the simulations.

Component	Unit	Value
Plant lifespan, n	year	30
Interest rate, i	%	5
Plant availability	%	90
MED plant, C_{MED}	$	$1082 + 2549 \times A(m^2)$
Crystallizer, C_{cryst}	$	$28531 \times ln\left[\dot{m}_{b,N}(m^3/day)\right] + 18824$
Land & site development, C_{ls}	$/(m^3/day)	25.31
Feed brine storage tank, C_{fst} /C_{bst}	$/m^3	95.42
Distillate storage, C_{dst}	$/m^3	75.66
Utility cost, C_{ut}	$/(m^3/day)	41.09
Other direct cost, C_{ot}	$/(m^3/day)	83.4
Steam, C_{th}	$/ton	8
Electricity, C_{el}	$/kWh	0.065
Labor, C_{la}	$/m^3	0.03
Chemical, C_{ch}	$/m^3	0.019
Equipment replacement & maintenance, C_{re}	$/(m^3/day)	0.02

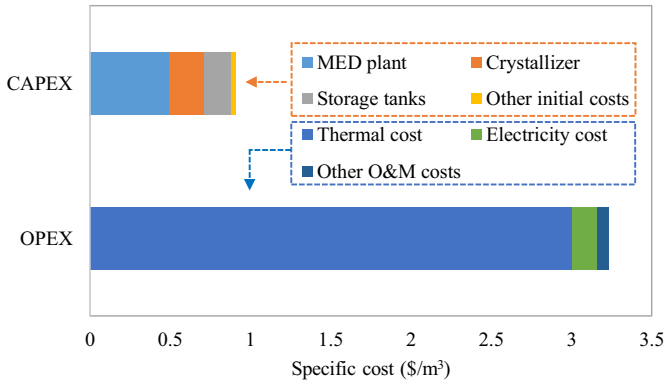

Fig. 10. Contribution of CAPEX and OPEX by different cost components.

The final cost is also subjected to the economic parameters, i.e. plant lifespan, plant availability, and interest rate. To investigate the impacts of these parameters, a sensitivity analysis is performed. The results are plotted in Fig. 13. Among different economic parameters, the final cost is the most sensitive to the interest rate, and a variation of ±3% in interest rate leads to ~$0.3/m^3 change of final cost under both scenarios. Moreover, reducing the plant lifespan from 30 to 20 years also increases the final cost by >$0.2/m^3. The cost is not sensitive to plant availability, and the change of cost is marginal at $0.05/m^3 when availability is varied by ±5%.

Fig. 14 compares the costs of different brine treatment methods. Under the regular scenario, the proposed ZLD system is only comparable with the evaporation ponds, while all the remaining methods are cheaper. Even when waste heat is available, the proposed system is still more expensive than most methods. However, it should be noted that these simple methods discharge brine directly to the environment without any treatment, whereas the proposed ZLD method and evaporation pond are environmentally benign due to zero waste discharge. Moreover, the proposed ZLD system can produce freshwater and salt crystals, and the revenue of selling these products can compensate for the high system cost and make the system profitable [19].

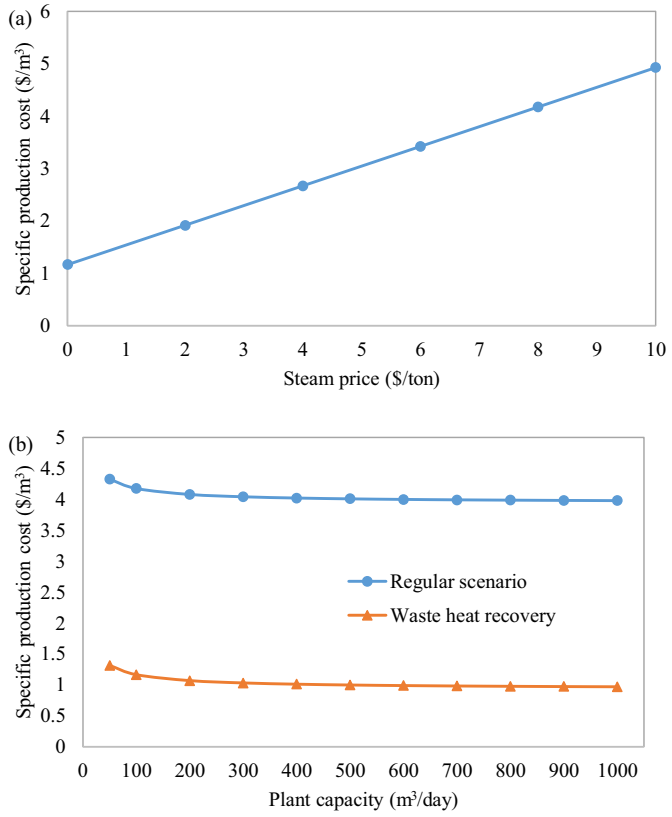

Fig. 11. Specific production cost under different (a) steam prices and (b) plant capacity.

4.3. Performance optimization

According to the results of the economic analysis, it can be concluded that a crucial way to improve the economic viability of the proposed ZLD system is to reduce the cost of thermal energy. However, thermal energy price is subjected to the availability of cost-effective heat sources. A more applicable solution is to reduce heat consumption via design optimization. In MED, reduction of heat consumption can be easily achieved via increasing the operating stages, but the initial plant cost will increase accordingly, as discussed above. When high-pressure steam is available, a more economical way is to employ a thermal vapor compressor (TVC), which can compress a portion of vapor from the condenser to a higher temperature so that it can be used as the heating medium. For the pressure gradient in the ZLD system, it is not difficult to design TVC with an entrainment ratio of >0.3 [38], which will lead to ~23% saving of steam consumption. Heat consumption can also be reduced by improving the crystallizer design. Currently, there is no heat recovery in the crystallizer and the condensation heat is wasted. If a multi-effect crystallizer can be designed to reuse the condensation heat, the system energy efficiency will be enhanced significantly, thus further reducing the thermal energy cost.

5. Conclusions

In this study, a hybrid system integrating multi-effect distillation (MED) and evaporative crystallization has been developed to treat the desalination brine and achieve zero liquid discharge (ZLD) status. A thermodynamic analysis is first performed to obtain its energy consumption, specific heat transfer area, and exergy efficiency under different design and operating conditions. Afterward, an economic analysis is conducted to evaluate the costs of the proposed ZLD system. Key findings from the current study are highlighted as follows:

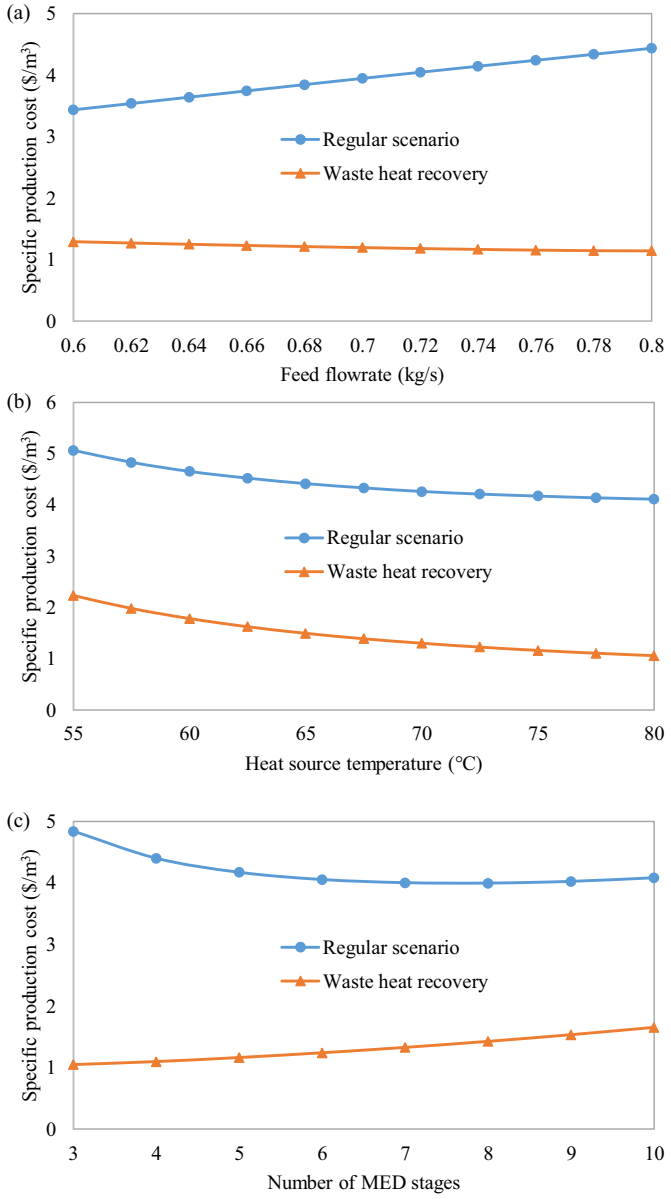

Fig. 12. Specific production cost under different (a) feed flowrate, (b) number of MED stages, and (c) heat source temperature.

(1) Specific heat consumption decreases significantly under more number of MED stages, while a higher heat source temperature reduces pumping power consumption;
(2) The specific heat transfer area for treating per kg/s of brine ranges between 110 and 340 m^2. The value is lower under a higher feed flowrate, a higher heat source temperature, and fewer MED stages;
(3) Second-law efficiency of the ZLD process is 10–17%, and it is promoted by lower feed flowrates, lower heat source temperature, and more numbers of MED stages;
(4) The cost of treating per m^3 of brine is $4.17, and ~$3/m^3 is contributed by thermal energy cost. When waste heat is available, the cost can be reduced to $1.16/$m^3$;
(5) The final cost can also be lowered by increasing the number of MED stages to reduce heat consumption as well as scaling up the plant;
(6) The proposed ZLD system is more cost-effective than the evaporation pond, and it is also comparable with the direct injection

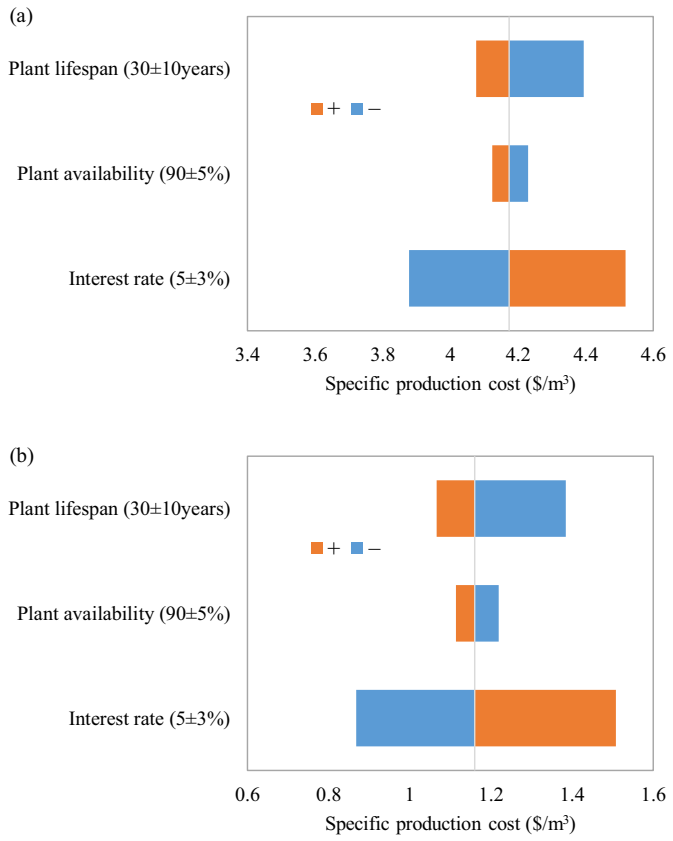

Fig. 13. Sensitivity analysis of production cost as a function of economic parameters under (a) regular scenario with a steam price of $8/ton, and (b) waste heat recovery.

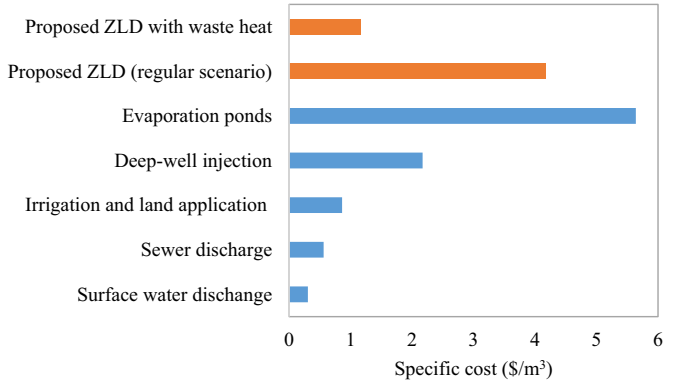

Fig. 14. Cost comparison between the proposed ZLD system and other brine treatment method.

methods when the profits of selling freshwater and salt are considered.

CRediT authorship contribution statement

Qian Chen: conceptualization, methodology, software, validation, formal analysis, writing - original draft;

Muhammad Burhan: formal analysis, investigation, validation;

Muhammad Wakil Shahzad: formal analysis, investigation, validation;

Doskhan Ybyraiymkul: formal analysis, validation;

Faheem Hassan Akhtar: formal analysis, validation;

Yong Li: formal analysis, validation;

Kim Choon Ng: conceptualization, formal analysis, supervision, project administration, funding acquisition.

Declaration of competing interest

The authors declare that they have no known competing financial interests or personal relationships that could have appeared to influence the work reported in this paper.

Acknowledgement

This research was supported by the Water Desalination and Reuse Center (WDRC), King Abdullah University of Science and Technology (KAUST).

Appendix A. Supplementary data

Supplementary data to this article can be found online at https://doi.org/10.1016/j.desal.2020.114928.

References

[1] Unies, N., *Water in a changing world. The United Nations World Water Development Report 3.* World Water Assessment Programme, En ligne. http://www.unesco.org/water/wwap/wwdr/wwdr3 (page consultée le 5 juillet 2009), 2009.
[2] Water, U., *2018 UN World Water Development Report, Nature-based Solutions for Water.* 2018.
[3] Virgili, F., T. Pankratz, and J. Gasson, *IDA Desalination Yearbook 2015–2016*. 2016: Media Analytics Limited.
[4] Shahzad, M.W., M. Burhan, and K.C. Ng, *Pushing desalination recovery to the maximum limit: membrane and thermal processes integration.* Desalination, 2017. **416**: p. 54–64.
[5] Chen, Q., Y. Li, and K. Chua, *On the thermodynamic analysis of a novel low-grade heat driven desalination system.* Energy Conversion and Management, 2016. **128**: p. 145–159.
[6] Chen, Q. and K.J. Chua, *A spray assisted low-temperature desalination technology*, in *Emerging technologies for sustainable desalination handbook*. 2018, Elsevier. p. 255–284.
[7] Giwa, A., V. Dufour, F. Al Marzooqi, M. Al Kaabi, and S. Hasan, *Brine management methods: recent innovations and current status.* Desalination, 2017. **407**: p. 1–23.
[8] Subramani, A. and J.G. Jacangelo, *Treatment technologies for reverse osmosis concentrate volume minimization: a review.* Separation and Purification Technology, 2014. **122**: p. 472–489.
[9] Petersen, K.L., A. Paytan, E. Rahav, O. Levy, J. Silverman, O. Barzel, D. Potts, and E. Bar-Zeev, *Impact of brine and antiscalants on reef-building corals in the Gulf of Aqaba–Potential effects from desalination plants.* Water research, 2018. **144**: p. 183–191.
[10] Missimer, T.M. and R.G. Maliva, *Environmental issues in seawater reverse osmosis desalination: intakes and outfalls.* Desalination, 2018. **434**: p. 198–215.
[11] Lu, K.J., Z.L. Cheng, J. Chang, L. Luo, and T.-S. Chung, *Design of zero liquid discharge desalination (ZLDD) systems consisting of freeze desalination, membrane distillation, and crystallization powered by green energies.* Desalination, 2019. **458**: p. 66–75.
[12] Nakoa, K., K. Rahaoui, A. Date, and A. Akbarzadeh, *Sustainable zero liquid discharge desalination (SZLDD).* solar Energy, 2016. **135**: p. 337–347.
[13] Guo, H., H.M. Ali, and A. Hassanzadeh, *Simulation study of flat-sheet air gap membrane distillation modules coupled with an evaporative crystallizer for zero liquid discharge water desalination.* Applied Thermal Engineering, 2016. **108**: p. 486–501.
[14] Guan, G., R. Wang, F. Wicaksana, X. Yang, and A.G. Fane, *Analysis of membrane distillation crystallization system for high salinity brine treatment with zero discharge using Aspen flowsheet simulation.* Industrial & engineering chemistry research, 2012. **51**(41): p. 13405–13413.
[15] Julian, H., S. Meng, H. Li, Y. Ye, and V. Chen, *Effect of operation parameters on the mass transfer and fouling in submerged vacuum membrane distillation crystallization (VMDC) for inland brine water treatment.* Journal of Membrane Science, 2016. **520**: p. 679–692.
[16] Creusen, R., J. van Medevoort, M. Roelands, A.V.R. van Duivenbode, J.H. Hanemaaijer, and R. van Leerdam, *Integrated membrane distillation–crystallization: process design and cost estimations for seawater treatment and fluxes of single salt solutions.* Desalination, 2013. **323**: p. 8–16.
[17] Edwie, F. and T.-S. Chung, *Development of simultaneous membrane distillation–crystallization (SMDC) technology for treatment of saturated brine.* Chemical Engineering Science, 2013. **98**: p. 160–172.
[18] Zhao, D., J. Xue, S. Li, H. Sun, and Q.-D. Zhang, *Theoretical analyses of thermal and economical aspects of multi-effect distillation desalination dealing with high-salinity wastewater.* Desalination, 2011. **273**(2–3): p. 292–298.

[19] Panagopoulos, A., *Process simulation and techno-economic assessment of a zero liquid discharge/multi-effect desalination/thermal vapor compression (ZLD/MED/TVC) system.* International Journal of Energy Research, 2020. **44**(1): p. 473–495.
[20] Onishi, V.C., A. Carrero-Parreno, J.A. Reyes-Labarta, E.S. Fraga, and J.A. Caballero, *Desalination of shale gas produced water: a rigorous design approach for zero-liquid discharge evaporation systems.* Journal of Cleaner Production, 2017. **140**: p. 1399–1414.
[21] Sharqawy, M.H., J.H. Lienhard, and S.M. Zubair, *Thermophysical properties of seawater: a review of existing correlations and data.* Desalination and water treatment, 2010. **16**(1–3): p. 354–380.
[22] Wagner, W. and H.-J. Kretzschmar, *IAPWS industrial formulation 1997 for the thermodynamic properties of water and steam.* International Steam Tables: Properties of Water and Steam Based on the Industrial Formulation IAPWS-IF97, 2008: p. 7–150.
[23] Sparrow, B.S., *Empirical equations for the thermodynamic properties of aqueous sodium chloride.* Desalination, 2003. **159**(2): p. 161–170.
[24] El-Dessouky, H., I. Alatiqi, S. Bingulac, and H. Ettouney, *Steady-state analysis of the multiple effect evaporation desalination process.* Chemical Engineering & Technology: Industrial Chemistry-Plant Equipment-Process Engineering-Biotechnology, 1998. **21**(5): p. 437–451.
[25] Luo, L., J. Chang, and T.-S. Chung, *Cooling crystallization of sodium chloride via hollow fiber devices to convert waste concentrated brines to useful products.* Industrial & Engineering Chemistry Research, 2017. **56**(36): p. 10183–10192.
[26] Bui, D.T., M.K. Ja, J.M. Gordon, K.C. Ng, and K.J. Chua, *A thermodynamic perspective to study energy performance of vacuum-based membrane dehumidification.* Energy, 2017. **132**: p. 106–115.
[27] Amelkin, S., A. Tsirlin, J. Burzler, S. Schubert, and K.-H. Hoffmann, *Minimal work for separation processes of binary mixtures.* Open Systems & Information Dynamics, 2003. **10**(04): p. 335–349.
[28] Chen, Q., M.K. Ja, Y. Li, and K. Chua, *Energy, economic and environmental (3E) analysis and multi-objective optimization of a spray-assisted low-temperature desalination system.* Energy, 2018. **151**: p. 387–401.
[29] Palenzuela, P., A.S. Hassan, G. Zaragoza, and D.-C. Alarcón-Padilla, *Steady state model for multi-effect distillation case study: plataforma Solar de Almería MED pilot plant.* Desalination, 2014. **337**: p. 31–42.
[30] Chen, Q., M.K. Ja, Y. Li, and K. Chua, *Energy, exergy and economic analysis of a hybrid spray-assisted low-temperature desalination/thermal vapor compression system.* Energy, 2019. **166**: p. 871–885.
[31] Chen, Q., M.K. Ja, Y. Li, and K. Chua, *On the second law analysis of a multi-stage spray-assisted low-temperature desalination system.* Energy Conversion and Management, 2017. **148**: p. 1306–1316.
[32] Mistry, K.H., R.K. McGovern, G.P. Thiel, E.K. Summers, S.M. Zubair, and J.H. Lienhard, *Entropy generation analysis of desalination technologies.* Entropy, 2011. **13** (10): p. 1829–1864.
[33] Chen, Q., M. Burhan, M.W. Shahzad, D. Ybyraiymkul, F.H. Akhtar, and K.C. Ng, *Simultaneous production of cooling and freshwater by an integrated indirect evaporative cooling and humidification-dehumidification desalination cycle.* Energy Conversion and Management, 2020. **221**: p. 113169.
[34] Al-Hengari, S., W. ElMoudir, and M.A. El-Bousiffi, *Economic assessment of thermal desalination processes.* Desalination and Water Treatment, 2015. **55**(9): p. 2423–2436.
[35] Elsayed, M.L., O. Mesalhy, R.H. Mohammed, and L.C. Chow, *Transient and thermo-economic analysis of MED-MVC desalination system.* Energy, 2019. **167**: p. 283–296.
[36] Papapetrou, M., A. Cipollina, U. La Commare, G. Micale, G. Zaragoza, and G. Kosmadakis, *Assessment of methodologies and data used to calculate desalination costs.* Desalination, 2017. **419**: p. 8–19.
[37] Christ, A., B. Rahimi, K. Regenauer-Lieb, and H.T. Chua, *Techno-economic analysis of geothermal desalination using hot sedimentary aquifers: a pre-feasibility study for Western Australia.* Desalination, 2017. **404**: p. 167–181.
[38] Power, R.B., *Steam jet ejectors for the process industries.[Glossary included].* 1994.